Higgs Candidate Property Measurements with the Compact Muon Solenoid

Andrew Whitbeck, on behalf of the CMS Collaboration
Department of Physics and Astronomy, Johns Hopkins University, Baltimore 21218, USA

Property measurements of the Higgs boson candidate are presented using proton-proton collision data collected with the Compact Muon Solenoid (CMS) detector corresponding to integrated luminosities of 5.1 fb^{-1} at $\sqrt{s}$=7 TeV and up to 19.6 fb^{-1} at $\sqrt{s}$=8 TeV. Combined mass measurements using the ZZ and $\gamma\gamma$ decay channels and consistency of couplings of the observed boson with respect to those predicted from the SM Higgs boson is tested using data corresponding to 5.1 fb^{-1} at $\sqrt{s}$=7 TeV and up to 12.2 fb^{-1} at $\sqrt{s}$=8 TeV. The spin-parity of the boson is studied using the ZZ and WW decay channels.

1 Introduction

The Standard Model (SM) of electroweak interaction[1,2,3] utilizes a complex doublet scalar field to spontaneously break electroweak symmetry in order for the weak gauge bosons to acquire mass and predicts a massive neutral scalar, the Higgs boson[4,5,6,7]. In July 2012, the CMS and ATLAS collaborations announced[8,9] the discovery of a new Higgs-like boson at a mass around 125 GeV. These proceedings present property measurements of this Higgs-like resonance using the CMS detector[10]. Combining different channels we present the mass measurement as well as the consistency of production and decay rates and couplings with respect to expectation from SM Higgs using 5.1 (12.2) fb^{-1} of data at $\sqrt{s}$ =7 (8) TeV. Finally, the consistency of data with respect several different spin-parity hypotheses is tested.

2 Combined properties

The combination of signal strength measurements in different channels can provide information about the properties of the observed resonance. In this section, results combining a number of channels to measure or constrain resonance properties are presented. These results were obtained using up to 5.1 (12.2) fb^{-1} of the 7 (8) TeV datasets[a]. The details of each individual channel can be found elsewhere[11,12,13,14,15,16,17].

2.1 Mass measurement

The measurement of the resonance mass is done by simultaneously fitting for the mass, m_X, and the signal strength, μ, in both the ZZ and $\gamma\gamma$ channels, the two high resolution decay channels. The 68% CL contours are shown as a function of μ and m_X in the left plot of figure 1. The red and green contours correspond to the individual scan in the ZZ and $\gamma\gamma$ channel respectively while the black is the combination of the two. The relative signal strength in the two channels is fixed to SM expectation.

[a]Results obtained from the $\gamma\gamma$ channel correspond to 5.3 fb^{-1} of the 8 TeV dataset.

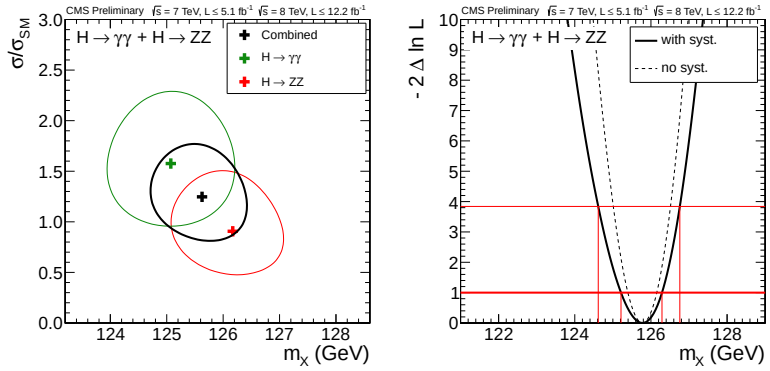

Figure 1: Distribution of -2ln$\mathscr{L}$ vs μ and m_X (left) for the $\gamma\gamma$ channel (green), the ZZ channel (red), and the combination of the two (black). The right plot shows the combination of the $\gamma\gamma$ and ZZ channels profiling the signal strength of each of channel.

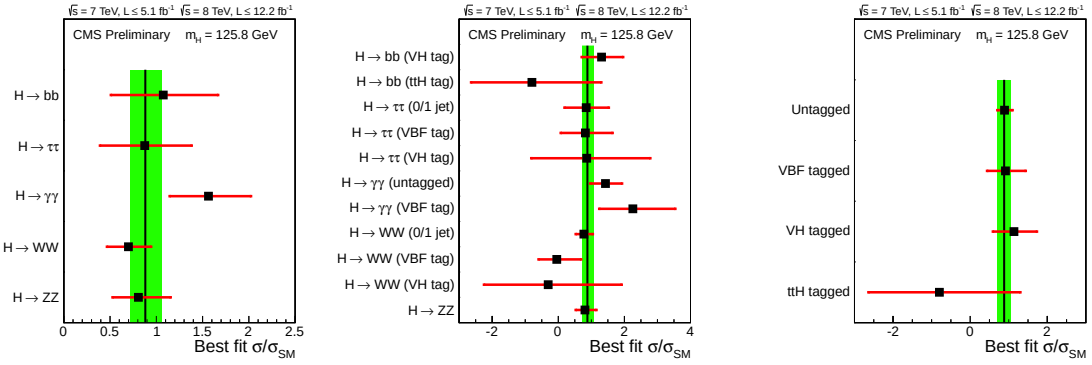

Figure 2: left: Values of μ for the combination (solid vertical line) and for sub-combinations grouped by decay mode (points). middle: Values of μ for the combination (solid vertical line) and for contributing channels (points). right: Values of μ for the combination (solid vertical line) and for sub-combinations grouped by a signature enhancing specific production mechanisms (points). The 68% CL interval is represented by the green band for the combination and the red bars for the sub-combinations.

To be more model independent, the 1D -2ln$\mathscr{L}$ scan of m_X is done by profiling μ separately in the ZZ channel as well as in the untagged and di-jet categories of the $\gamma\gamma$ channel. The 1D -2ln$\mathscr{L}$ scan for this measurement is shown in the right plot of figure 1 and the 68% CL interval is found to be $m_X = 125.8 \pm 0.4$ (stat) ± 0.4 (syst) GeV.

2.2 Signal strengths

The compatibility of the observed excess with the SM Higgs prediction can be first assessed by measuring the combined signal strength and the signal strength channel by channel. Figure 2 shows the 68% CL interval of the combined signal strength, green band, and the 68% CL interval of the signal strength measured by individual channels. All channels individually as well as the combination of all channels are consistent with SM expectation. The 68% CL interval for the combined signal strength is found to be 0.88 ± 0.21 when $m_X = 125.8$ GeV.

2.3 Compatibility of data with SM Higgs couplings

The total event yield in any channel can be related to the partial and total width of the Higgs as follows

$$N(xx \to H \to yy) \sim \sigma(xx \to H) \times \mathscr{B}(H \to yy) \sim \frac{\Gamma_{xx}\Gamma_{yy}}{\Gamma_{tot}}.$$

Thus, there are eight parameters, $\Gamma_{WW}, \Gamma_{ZZ}, \Gamma_{tt}, \Gamma_{bb}, \Gamma_{\tau\tau}, \Gamma_{gg}, \Gamma_{\gamma\gamma}, \Gamma_{tot}$, which describe the rates of the current searches. Testing for possible deviations from SM Higgs expectations can be

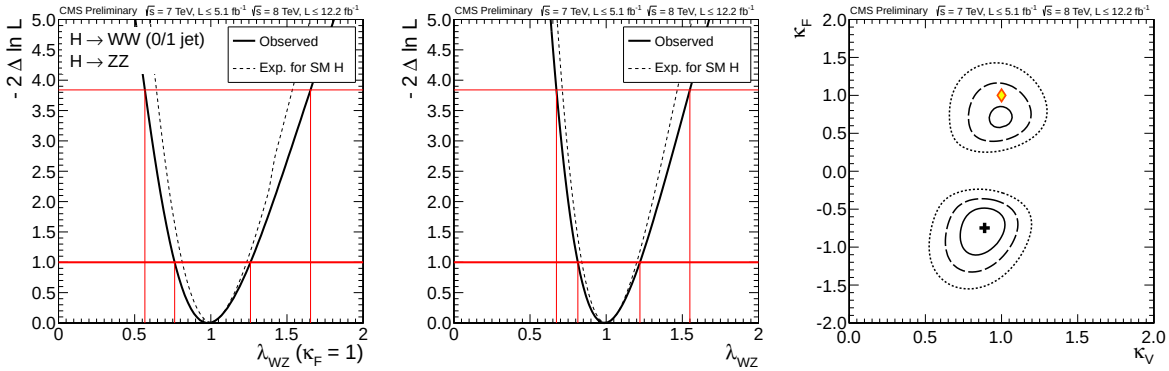

Figure 3: left: 1D test statistics q(λ_{WZ}) scan vs the coupling modifier ratio λ_{WZ}, profiling the coupling modifier κ_Z and all other nuisances. The coupling to fermions is taken to be the SM one ($\kappa_f = 1$). middle: 1D test statistics q(λ_{WZ}) scan vs the coupling modifier ratio λ_{WZ}, profiling the coupling modifiers κ_Z and κ_f and all other nuisances. right: 2D test statistics q(κ_V, κ_f) scan. Solid, dashed, and dotted contour represent the 68%, 95%, and 99.7% CL areas.

formulated in terms of scale factors, κ_i, which represent deviations with respect to the SM Higgs partial widths, e.g. $\kappa_W^2 = \Gamma_{WW}/\Gamma_{WW}^{SM}$. Any deviations from $\kappa_i = 1$ would imply physics beyond the SM. The measurements presented in this section are following the prescription of the LHC Higgs Cross Section Working Group[21].

By requiring an approximate custodial symmetry, tree-level relations between the W and Z masses as well as the W and Z couplings to the Higgs boson can be protected against large radiative corrections. Thus, large discrepancies of the ratio of the W and Z couplings to Higgs are an indication of physics beyond the standard model. To test this, we fit for the ratio $\lambda_{WZ} = \kappa_W/\kappa_Z$. In order to properly account for small differences in the VBF fraction between the $H \to ZZ$ and $H \to WW$ channels, κ_Z is profiled. The fits are then done in two different ways, using only the $H \to ZZ$ and $H \to WW$ channels, left plot of figure 3, and using all channels profiling κ_f[b] in addition to κ_Z, middle plot of figure 3. We find that in both cases λ_{WZ} is consistent with SM expectation and fix it to unity for all subsequent measurements. The 95% CL interval for λ_{WZ} using the ZZ and WW channels is [0.57,1.65], and [0.67,1.55] using the combination of all channels.

We also test the compatibility of data with respect to the SM Higgs using two parameters, κ_v and κ_f, which are scaling factors for all W/Z couplings and fermionic couplings respectively. Since $\Gamma_{\gamma\gamma}$ is induced via a W and top loop, it scales as $|\alpha\kappa_V + \beta\kappa_f|^2$. As such, the $\gamma\gamma$ channel is the only channel sensitive to the relative sign between κ_V and κ_f. The right plot of figure 3 shows the -2ln$\mathscr{L}$ scan vs κ_V, κ_f. The global minimum lies in the (+,-) quadrant because of the excess in the $\gamma\gamma$ channel. However, the data is still consistent with the standard model within 2σ. Fixing κ_V (κ_f) to unity, the 95% CL interval for κ_f (κ_V) is found to be [0.40,1.12] ([0.78,1.19]).

Since $H \to\gamma\gamma$ and $gg \to H$ are induced through loops, κ_γ and κ_g are sensitive to the presence of new particles. The left plot of figure 4 shows the -2ln$\mathscr{L}$ scan for κ_γ and κ_g and is consistent with the SM to within 2σ. Profiling either κ_γ (κ_g), we find that the 95% CL interval for κ_g (κ_γ) is [0.55,1.07] ([0.98,1.92]). BSM decay channels can be probed by fitting for $BR_{BSM} = \Gamma_{BSM}/\Gamma_{tot}$. When profiling κ_γ and κ_g the 95% CL interval for BR_{BSM} is found to be [0.00,0.62].

We can also test for asymmetries between either quark and lepton or up-type and down-type fermions. These deviation can occur in different flavors of two Higgs doublet models. Two ratios are constructed to test these hypotheses, $\lambda_{du} = \kappa_d/\kappa_u$ and $\lambda_{\ell q} = \kappa_\ell/\kappa_q$. The middle plot of figure 4 shows the -2ln$\mathscr{L}$ scan vs λ_{du} with κ_V and κ_u profiled. The 95% CL interval for λ_{du} is [0.45,1.66]. The right plot of figure 4 shows the -2ln$\mathscr{L}$ scan vs $\lambda_{\ell q}$ with κ_V and κ_q profiled. The

[b] κ_f is a single modifier for all couplings to fermions

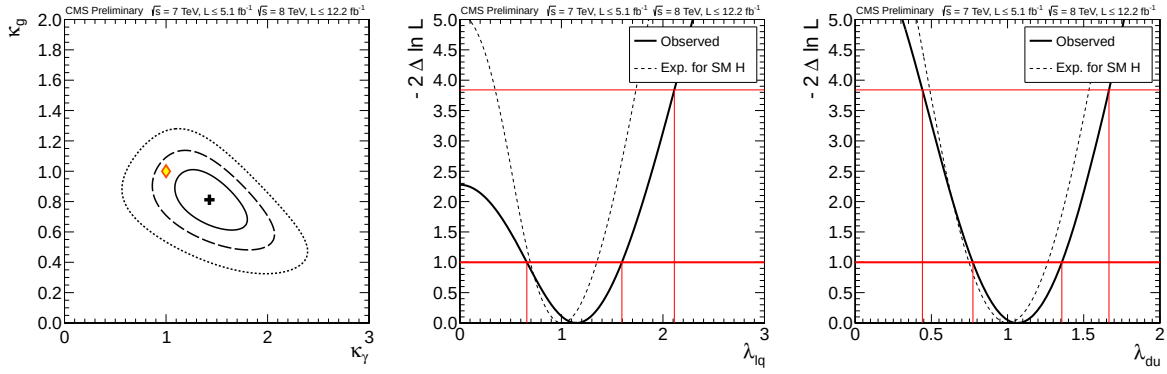

Figure 4: left: 2D test statistics q(κ_g, κ_γ) scan assuming that $\Gamma_{BSM} = 0$. Solid, dashed, and dotted contours show the 68%, 95%, and 99.7% CL ranges. middle: 1D test statistics q(λ_{du}) scan vs the coupling modifier ratio λ_{du}, profiling the coupling modifiers κ_u and κ_V and all other nuisances. κ_u, and κ_V are always taken to be positive. right: 1D test statistics q($\lambda_{\ell q}$) scan vs the coupling modifier ratio $\lambda_{\ell q}$, profiling the coupling modifiers κ_u and κ_V and all other nuisances. κ_q, and κ_V are always taken to be positive.

J^P	production	comment	expect ($\mu = 1$)	obs. 0^+	obs. J^P	CL_s
0^-	$gg \to X$	pseudoscalar	$2.6\sigma(2.8\sigma)$	0.5σ	3.3σ	0.16%
0_h^+	$gg \to X$	higher dim operator	$1.7\sigma(1.8\sigma)$	0.0σ	1.7σ	8.1%
2_{mgg}^+	$gg \to X$	minimal couplings	$1.8\sigma(1.9\sigma)$	0.8σ	2.7σ	1.5%
2_{mqq}^+	$q\bar{q} \to X$	minimal couplings	$1.7\sigma(1.9\sigma)$	1.8σ	4.0σ	$< 0.1\%$
1^-	$q\bar{q} \to X$	exotic vector	$2.8\sigma(3.1\sigma)$	1.4σ	$> 4.0\sigma$	$< 0.1\%$
1^+	$q\bar{q} \to X$	exotic pseudovector	$2.3\sigma(2.6\sigma)$	1.7σ	$> 4.0\sigma$	$< 0.1\%$

Table 1: List of models used in analysis of spin-parity hypothesis corresponding to the pure states of the type noted. The expected separation is quoted for two scenarios, when the signal strength for each hypothesis is pre-determined from the fit to data and when events are generated with SM expectation for the signal yield ($\mu = 1$). The observed separation quotes consistency of the observation with the 0^+ model or J^P model, and corresponds to the scenario when the signal is pre-determined from the fit to data. The last column quotes the CL_s criterion for the J^P models.

95% CL interval for $\lambda_{\ell q}$ is [0.00,2.11]. Both measurements are consistent with SM expectation.

3 Spin-Parity

Understanding the spin and quantum numbers of the new boson is an important check of the SM. Different J^P quantum numbers and different couplings manifest themselves in the angular and mass correlations of di-boson decays allowing ZZ and WW events to be used to constrain the spin and parity of the boson. Using hypothesis testing, we evaluated the consistency of data with respect to either the SM Higgs hypothesis or six alternative J^P hypotheses. The alternative models tested are outline in Table 1 and discussed in detail elsewhere[20]. Results presented in this section are using up to 5.1 (19.6) fb^{-1} for the 7 (8) TeV dataset.

3.1 ZZ

The ZZ spin-parity analysis is done using a 2D unbinned likelihood to describe data. Analogous to how the signal strength measurement is performed[18], events are described using two variables. The first variable is a kinematic discriminant (KD) to separate signal from background, D_{bkg}, built from the combination of $m_{4\ell}$ and the KD used in the signal strength measurements[18]. The second is a KD which separates SM Higgs from some alternative J^P signal and is built from the seven dimensional probability for either SM Higgs, P_{SM}, or an alternative model, P_{JP},

$$D_{J^P} = \frac{P_{SM}}{P_{SM}+P_{JP}} = [1 + \frac{P_{SM}(m_{Z_1},m_{Z_2},\vec{\Omega};m_{4\ell})}{P_{JP}(m_{Z_1},m_{Z_2},\vec{\Omega};m_{4\ell})}]^{-1},$$

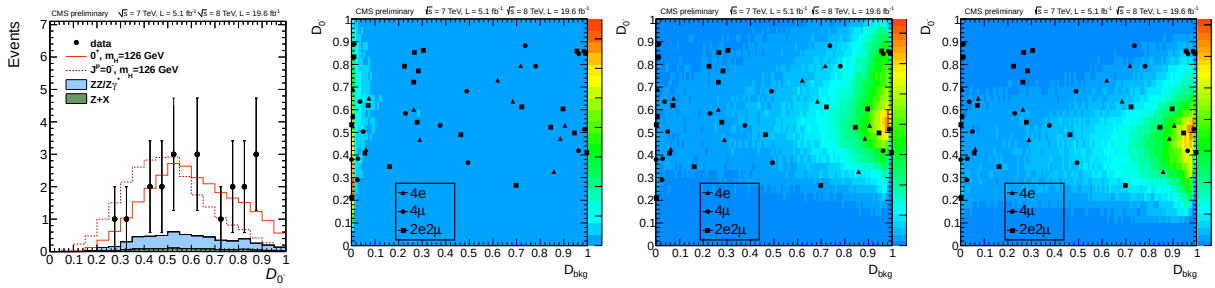

Figure 5: Distributions of D_{JP} with the requirement $D_{bkg} > 0.5$. Distributions in data (points with error bars) and expectations for background and signal are shown.Distributions of D_{0-} vs D_{bkg} for background (left), SM Higgs (middle), and pseudoscalar (right). MC expectation is represented by the color map while data is represented by black points.

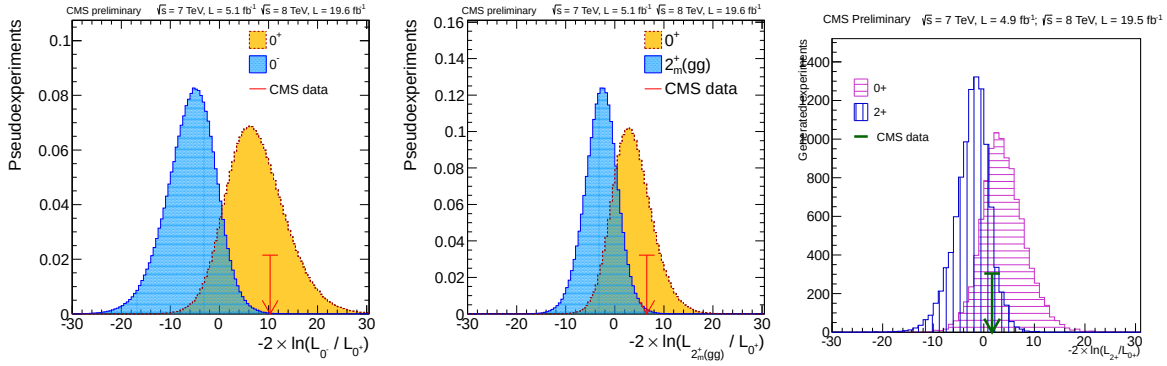

Figure 6: left,middle: Distribution test statistic for two signal types (0^+, yellow histogram, and J^P, blue histogram) for $m_H = 126$ GeV. Separation between 0^+ and 0^- (2^+_{mgg}) is shown on the left (middle). The arrow indicates the observed q-value. right: Distribution of test statistic, q, for SM Higgs hypothesis (purple histogram) and minimal coupling graviton hypothesis (blue histogram). Green arrow shows the q-value for data.

where Ω represents the five decay angles. The D_{0-} distributions after selecting events where $D_{bkg} > 0.5$ are shown in figure 5 along with the 2D distributions D_{bkg} vs. D_{0-} for background, SM Higgs, and pseudoscalar MC. All distributions are shown in the mass range 106< $m_{4\ell}$ <141 GeV.

Hypothesis tests were performed testing the SM Higgs hypothesis against each of the six alternative hypotheses, J^P=$0^-, 0^+_h, 1^+, 1^-, 2^+_{mgg}, 2^+_{mq\bar{q}}$. Toys were generated according to each hypothesis assuming either the SM Higgs cross section ($\mu = 1$) or using the best-fit signal strength from data for each hypothesis. The test statistic (q = -2ln($\mathscr{L}_{JP}/\mathscr{L}_{SM}$)) distributions for each measurement are shown in figure 6. A CL$_s$ criterion is defined as

$$\text{CL}_s = \mathscr{P}(q \geq q_{obs}|J^P)/\mathscr{P}(q \geq q_{obs}|SM).$$

Table 1 shows the expected separation, the observed separation assuming either the J^Por the 0^+ hypothesis, and the CL$_s$ value for each of the six alternative hypotheses. The expected separations range from 1.7-2.8σ while the CL$_s$ values range from 0.1%-10% when generating toys from the best-fit μ.

A fit for the continuous parameter, f_{a3}, was also performed. This parameter represents the amount of CP-violation present in data and can be defined as

$$f_{a3} = |A_3|^2/(|A_1|^2 + |A_3|^2).$$

A_1, A_2, and A_3 are defined in terms of the most general amplitude for a scalar decaying to two vector bosons,

$$A = v^{-1}\epsilon_1^{*\mu}\epsilon_2^{*\nu}(a_1 g_{\mu\nu} m_H^2 + a_2 q_\mu q_\nu + a_3 \epsilon_{\mu\nu\alpha\beta} q_1^\alpha q_2^\beta) = A_1 + A_2 + A_3,$$

where ϵ_i are the Z boson polarization vectors, q_i the Z boson momenta, a_i couplings, m_H the mass of the resonance, and $\epsilon_{\mu\nu\alpha\beta}$ the Levi-Civita tensor. In this measurement, we fix $A_2 = 0$.

Non-zero contributions from the A_3 term imply f_{a3} will be non-zero while if the resonance is either a pure SM Higgs (pseudoscalar), f_{a3} would be 0 (1). It should be stressed that f_{a3} is not a parameter which defines the mixture of parity-even and parity-odd states. The latter would require a model-dependent interpretation of the f_{a3} measurement. The best-fit value is found to be f_{a3}=$0.00^{+0.23}_{-0.00}$ and the 95% CL interval is [0.0,0.58].

3.2 WW

The WW spin-parity analysis is done using a 2D binned likelihood, $m_{\ell\ell}$ vs m_T[19], to describe data. The SM Higgs hypothesis is tested only against the minimal coupling graviton model produced through gluon-gluon fusion, $J^P = 2^+_{mgg}$. Distributions of the test statistic q = -2ln($\mathscr{L}_{2^+_{mgg}}/\mathscr{L}_{SM}$) are shown for SM Higgs hypothesis (purple) and the alternative hypothesis (blue) in the right plot of figure 6. The expected separation is 1.9 σ while the observed significance is 1.3 (0.9) σ with respect to the 2^+_{mgg} (0^+) hypothesis, slightly disfavoring the 2^+_{mgg} hypothesis, which corresponds to a CL$_s$ value of 12% when generating toys from the best-fit μ.

4 Conclusions

Property measurements have been presented for the Higgs-like resonance. The best-fit mass is found to be 125.8 ±0.4(stat) ±0.4 (syst) GeV. The best-fit signal strength combining all channels is found to be 0.88 ±0.21 measured at the best-fit mass. The consistency of the couplings of the observed boson with respect to SM Higgs expectation is tested in various ways and no significant deviation is found.

Consistency of kinematic distributions with respect to either the SM Higgs hypothesis and several alternative signal hypotheses of various spin and parity has been tested. In all cases, data is found to disfavor the alternative hypotheses. We find that data disfavors the 0^-, 2^+_{mgg}, 2^+_{mqq}, 1^+, and 1^- hypotheses at more than 2σ.

References

1. S. L. Glashow, Nucl. Phys. **22**, 579 (1961).
2. S. Weinberg, Phys. Rev. Lett. **19**, 1264 (1967).
3. A. Salam, Conf. Proc. C **680519**, 367 (1968).
4. F. Englert and R. Brout, Phys. Rev. Lett. **13**, 321 (1964).
5. P. W. Higgs, Phys. Lett. **12**, 132 (1964).
6. P. W. Higgs, Phys. Rev. Lett. **13**, 508 (1964).
7. G. S. Guralnik, C. R. Hagen and T. W. B. Kibble, Phys. Rev. Lett. **13**, 585 (1964).
8. S. Chatrchyan *et al.* [CMS], Phys. Lett. B **716**, 30 (2012) [arXiv:1207.7235 [hep-ex]].
9. G. Aad *et al.* [ATLAS], Phys. Lett. B **716**, 1 (2012) [arXiv:1207.7214 [hep-ex]].
10. S. Chatrchyan *et al.* [CMS], JINST **3**, S08004 (2008).
11. CMS Collaboration, CMS-PAS-HIG-12-015 (2012).
12. CMS Collaboration, CMS-PAS-HIG-12-044 (2012).
13. CMS Collaboration, CMS-PAS-HIG-12-043 (2012).
14. CMS Collaboration, CMS-PAS-HIG-12-051 (2012).
15. CMS Collaboration, CMS-PAS-HIG-11-024 (2011).
16. CMS Collaboration, CMS-PAS-HIG-12-003 (2012).
17. CMS Collaboration, CMS-PAS-HIG-12-041 (2012).
18. CMS Collaboration, CMS-PAS-HIG-13-002 (2013).
19. CMS Collaboration, CMS-PAS-HIG-13-003 (2013).
20. S. Bolognesi et al. Phys. Rev. D **86**, 095031 (2012) [arXiv:1208.4018 [hep-ph]].
21. LHC Higgs Cross Section Working Group et al., arxiv::1209.0040